

# Molecular imaging of nuclear factor-Y transcriptional activity maps proliferation sites in live animals

Frauke Goeman<sup>a,\*†</sup>, Isabella Manni<sup>a,\*</sup>, Simona Artuso<sup>a,\*</sup>, Balaji Ramachandran<sup>b</sup>, Gabriele Toietta<sup>c</sup>, Gianluca Bossi<sup>a</sup>, Gianpaolo Rando<sup>b</sup>, Chiara Cencioni<sup>d</sup>, Sabrina Germoni<sup>e</sup>, Stefania Straino<sup>c</sup>, Maurizio C. Capogrossi<sup>c</sup>, Silvia Bacchetti<sup>a</sup>, Adriana Maggi<sup>b</sup>, Ada Sacchi<sup>a</sup>, Paolo Ciana<sup>b</sup>, and Giulia Piaggio<sup>a</sup>

<sup>a</sup>Experimental Oncology Department, Istituto Regina Elena, 00158 Rome, Italy; <sup>b</sup>Department of Pharmacological Sciences, University of Milan, 20133 Milan, Italy; <sup>c</sup>Laboratorio di Patologia Vascolare, Istituto Dermatologico dell'Immacolata, IRCCS, 00167 Rome, Italy; <sup>d</sup>Laboratorio di Biologia Vascolare e Medicina Rigenerativa, Centro Cardiologico, Monzino-IRCCS, 20138 Milan, Italy; <sup>e</sup>SAFU, Istituto Regina Elena, 00158 Rome, Italy

**ABSTRACT** In vivo imaging involving the use of genetically engineered animals is an innovative powerful tool for the noninvasive assessment of the molecular and cellular events that are often targets of therapy. On the basis of the knowledge that the activity of the nuclear factor-Y (NF-Y) transcription factor is restricted in vitro to proliferating cells, we have generated a transgenic reporter mouse, called MITO-Luc (for mitosis-luciferase), in which an NF-Y-dependent promoter controls luciferase expression. In these mice, bioluminescence imaging of NF-Y activity visualizes areas of physiological cell proliferation and regeneration during response to injury. Using this tool, we highlight for the first time a role of NF-Y activity on hepatocyte proliferation during liver regeneration. MITO-Luc reporter mice should facilitate investigations into the involvement of genes in cell proliferation and provide a useful model for studying aberrant proliferation in disease pathogenesis. They should be also useful in the development of new anti/proproliferative drugs and assessment of their efficacy and side effects on nontarget tissues.

## Monitoring Editor

William P. Tansey  
Vanderbilt University

Received: Jan 19, 2012

Revised: Feb 10, 2012

Accepted: Feb 22, 2012

This article was published online ahead of print in MBoC in Press (<http://www.molbiolcell.org/cgi/doi/10.1091/mbc.E12-01-0039>) on February 29, 2012.

\*These authors contributed equally to this work. F.G. and I.M. conceived and designed the experiments. F.G., I.M., S.A., B.R., G.T., G.B., G.R., S.G., C.C., and S.S. performed the experiments. S.B. contributed to the conceptual framework of the manuscript. M.C., A.M., and A.S. contributed to the interpretation of the data. P.C. and G.P. designed and supervised the project. I.M., S.B., and G.P. wrote the paper.

<sup>†</sup>Present address: Translational Oncogenomics Unit, Istituto Regina Elena, 00144 Rome, Italy.

The authors declare no conflict of interest.

Address correspondence to: Giulia Piaggio ([piaggio@ifo.it](mailto:piaggio@ifo.it)) or Paolo Ciana ([paolo.ciana@unimi.it](mailto:paolo.ciana@unimi.it)).

Abbreviations used: 5-FU, 5-fluorouracil; Ad-dnYA, adenovirus dominant-negative nuclear factor-Y; Ad-NFYA, wild-type NF-YA; BLI, bioluminescence imaging; CCD, charge-coupled device; DAPI, 4',6-diamidino-2-phenylindole; DMBA, 7,12-dimethylbenz(a)anthracene; dpc, day postcoitum; ES, embryonic stem cell; FACS, fluorescence-activated cell sorting; GFP, green fluorescent protein; HSC, hematopoietic stem cell; MCTX, modified cobra toxin; MEF, mouse embryonic fibroblasts; MHC, myosin heavy chain; MITO-Luc, mitosis-luciferase; NF-Y, nuclear factor-Y; SC, satellite cell; TPA, phorbol ester 12-O-tetradecanoylphorbol-13 acetate.

© 2012 Goeman et al. This article is distributed by The American Society for Cell Biology under license from the author(s). Two months after publication it is available to the public under an Attribution–Noncommercial–Share Alike 3.0 Unported Creative Commons License (<http://creativecommons.org/licenses/by-nc-sa/3.0>). "ASCB®," "The American Society for Cell Biology®," and "Molecular Biology of the Cell®" are registered trademarks of The American Society of Cell Biology.

## INTRODUCTION

Nuclear factor-Y (NF-Y) is a trimeric activator composed of NF-YA, NF-YB, and NF-YC subunits, all of which are required for DNA binding. The three subunits are highly conserved in evolution and represent the complex recognizing the CCAAT motif (Dolfini et al., 2009). The NF-Y complex supports proliferation regulating the basal transcription of regulatory genes responsible for cell cycle progression, among which are mitotic cyclin complexes (Bolognese et al., 1999; Caretti et al., 1999; Farina et al., 1999; Sciortino et al., 2001; Gurtner et al., 2003, 2008; Di Agostino et al., 2006). We provide evidence that NF-Y plays a central role in the switch from proliferation to differentiation. In proliferating skeletal muscle cells, all subunits are expressed, whereas in terminally differentiated cells, NF-YA is undetectable, and the suppression of NF-Y function is crucial for the inhibition of multiple cell cycle genes and the induction of early muscle differentiation markers (Farina et al., 1999; Gurtner et al., 2008; Manni et al., 2008). In line with this, conditional deletion of NF-YA in mice causes early embryo lethality, demonstrating that NF-Y is essential for early mouse development (Bhattacharya et al., 2003). Moreover, it has been described that inhibition of NF-Y function leads to defects in embryonic (ES) and hematopoietic (HSC) stem cell proliferation (Grskovic et al., 2007; Bungartz et al., 2012).

Bioluminescence imaging (BLI) strategies have recently been incorporated into animal research protocols, including those involving the use of genetically engineered animals. These tools offer the advantage of noninvasive *in vivo* assessment of the molecular and cellular events that are often targets of therapy; as such, these events can be studied in individual animals over time. This reduces the number of animals required for a given study and improves the data set, as the temporal data allow for each animal to serve as its own internal control. For small rodents, such as mice, this noninvasive imaging technique allows detection of signals throughout the entire animal (Ciana *et al.*, 2003; Signore *et al.*, 2010).

In this paper, we present a new transgenic mouse model, MITO-Luc (for mitosis-luciferase) reporter mice, in which we demonstrate that proliferation can be visualized noninvasively *in vivo*. We based our model on the rationale that NF-Y activity is exerted only in proliferating cells. The transgenic mouse model we have developed harbors a strictly NF-Y-dependent promoter in front of a luciferase reporter, allowing us to monitor the NF-Y activity in a spatiotemporal manner within the entire living organism. Using a dominant-negative protein for NF-Y, we reveal for the first time a possible involvement of NF-Y activity in liver regeneration.

## RESULTS

### NF-Y-dependent cyclin B2 promoter fragment drives transcription in MITO-Luc mice

For the generation of the MITO-Luc reporter mice, we used a transgene harboring the luciferase gene under control of an NF-Y-dependent cyclin B2 promoter fragment as a sensor of NF-Y activity *in vivo*. To minimize the influence of the surrounding chromatin status at the integration site, we flanked this construct with insulators that were reported to overcome position effects to a large extent (Ciana *et al.*, 2003; Figure 1a). As a control, we cloned the same promoter regions with all CCAAT boxes mutated (CCAAT mutated into TTACT). To test the functionality of these constructs, we performed transient transfections in murine C2C12 (Figure 1b) and NIH 3T3 cells (unpublished data). These experiments revealed that the mutation of the CCAAT boxes led to a significant reduction of luciferase units, showing the dependency of this promoter construct on NF-Y activity. The transgene was injected in the pronucleus of fertilized C57BL/6xDBA/2 eggs using standard protocols (Hogan *et al.*, 1994). We obtained three independent founder animals, of which two were fertile. Semi-quantitative PCR analysis with genomic DNA from tail biopsies showed clear differences in the transgene amount in the two lines, #10 and #26 (Supplemental Figure S1). We injected the luciferase substrate  $\rho$ -luciferin, into anesthetized transgenic mice and visualized luciferase activity with a charge-coupled device (CCD) camera (Signore *et al.*, 2010). Both male and female mice were imaged in ventral and dorsal positions (Figure 1c). Light emission, although to different extents, was detected in areas corresponding to femur, skull, sternum, vertebral column, and spleen, and it was equal in both genders for common tissues. In males, testes were also luminescent (Figure S2A).

*In vivo* imaging is carried out in two dimensions; thus the definition of the organ/tissue contributing to the photon emission is limited; furthermore, tissue penetration can cause some emitted light to be lost. Therefore we carried out *ex vivo* experiments in which we measured luciferase activity of dissected organs from the killed mice. The measurement of the enzyme activity was done by bioluminescence, exposing the dissected organ to the CCD camera. As seen *in vivo*, overall light emission was equal in both genders (unpublished data). As shown in Figure 1d, luciferase activity, as measured *ex vivo*, generally reproduces and extends what is observed *in vivo*. Indeed,

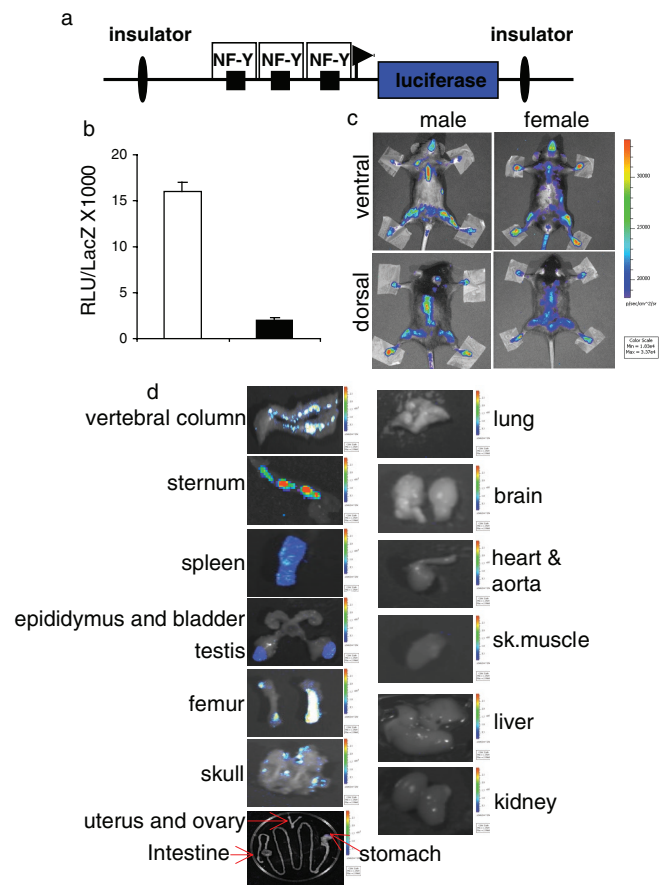


**FIGURE 1:** NF-Y-dependent luciferase transcription in MITO-Luc mice. (a) Scheme of the transgene used. (b) C2C12 cells transiently transfected with the wild-type (white bar) or mutated (black bar) CCAAT (CCAAT versus TTACT) boxes. Transfection efficiency was normalized with cotransfected  $\beta$ -galactosidase expression vector (pCMV-lacZ). The error bars indicate the deviation of the mean of two experiments performed in triplicate. (c) BLI of representative MITO-Luc mice. The images were collected on 31 animals of each gender; one representative animal is shown. (d) *Ex vivo* BLI of positive and negative luciferase organs. After the animals were killed, the indicated organs were collected. Images of five animals for each gender were collected and one representative animal is shown. (c and d) Light emitted from the animal appears in pseudocolor scaling.

we detected high luciferase activity in the vertebral column, sternum, spleen, testis, femur, and skull as expected, based on *in vivo* analysis. Several tissues (e.g., lung, brain, heart, aorta, skeletal muscle, liver, and kidney) did not emit light. All the tissues noted were imaged with the same color scale bar. In these experimental conditions, the intestine, stomach, uterus, and ovaries also did not emit light. Interestingly, using a more stringent color scale bar, we also observed luciferase activity along these tissues, suggesting that their lower luminescence *in vivo* was indeed due to tissue penetration light loss. To demonstrate that these signals were specific, we imaged the spleen and the lung with the same color scale bar as negative and positive tissues, respectively (Figure S2B).

To further verify tissue distribution of luciferase, we measured enzymatic activity in homogenates of 21 different tissues from both male and female 6- to 8-wk-old mice (Figure S3). The *in vitro* results closely resembled those seen *in vivo* and *ex vivo*. Transgenic line #26 showed similar *in vivo*, *ex vivo*, and *in vitro* results but with lower intensities (unpublished data), due to its lower transgene copy number.

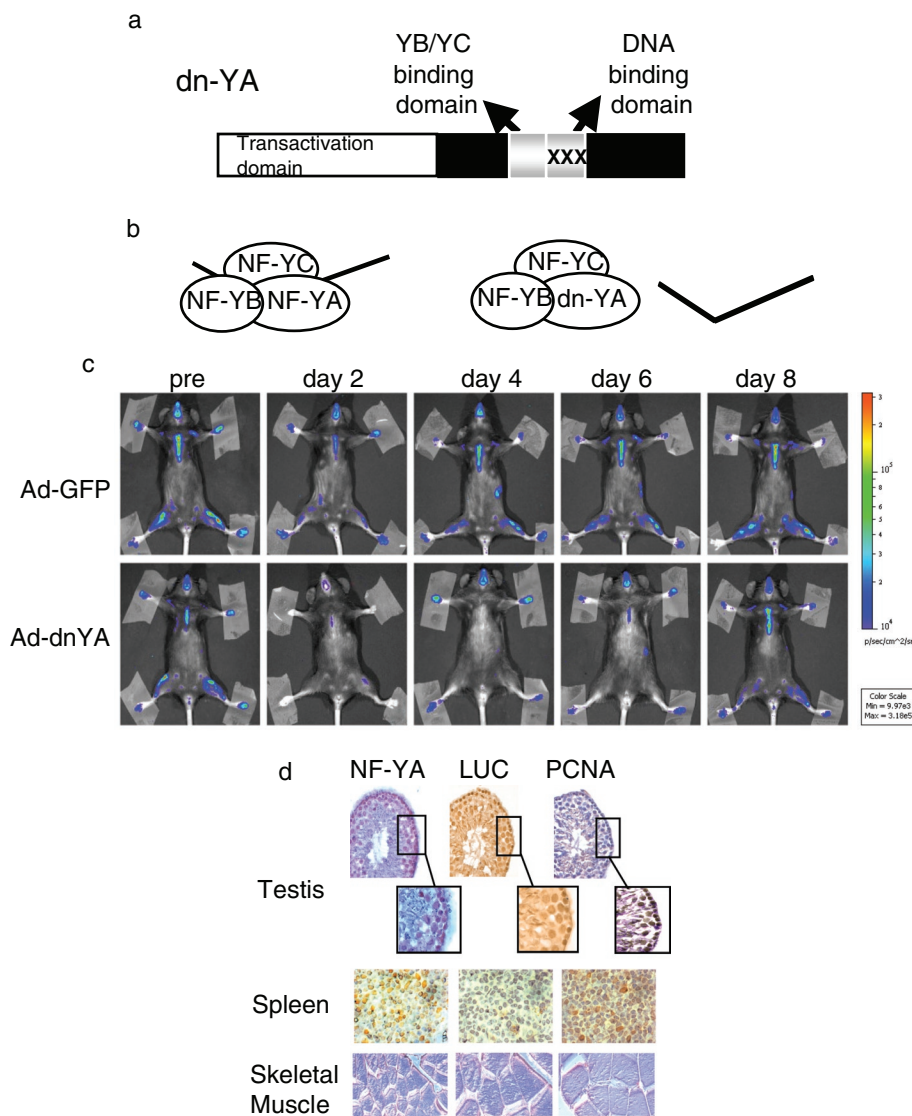


**FIGURE 2:** NF-Y–dependent luciferase transcription in MITO-Luc mice. (a) Scheme of the dominant-negative NF-YA protein (dn-YA). (b) The NF-Y subunits, A, B, and C, form a complex that binds DNA. dn-YA is still able to interact with the NF-YB-/YC dimer, but the resulting trimer is inactive in terms of DNA binding. (c) BLI of representative MITO-Luc mice before (pre) and after (days 2, 4, 6, 8) injection of an adenovirus vector expressing GFP (Ad-GFP) or Ad-dnYA. The experiments were conducted on nine animals per group. Light emitted from the animals appears in pseudocolor scaling. (d) Immunohistochemical analysis of NF-YA, luciferase (LUC), and PCNA in testis (40 $\times$ ; insets: 100 $\times$ ), spleen (100 $\times$ ), and skeletal muscle (60 $\times$ ) tissues from a representative MITO-Luc mouse.

To demonstrate the dependence of luciferase expression on NF-Y transcriptional activity, we injected MITO-Luc mice intravenously with an adenovirus expressing a dominant-negative mutant of NF-Y, dn-YA (Ad-dnYA), that impairs the DNA binding of the resulting complex (Mantovani *et al.*, 1994; Gurtner *et al.*, 2008). This molecule is an NF-YA protein with a triple amino acid substitution in the DNA-binding domain that impairs its ability to bind DNA (Figure 2a). It is still able to interact with an NF-YB-/YC dimer, but the resulting trimer is inactive in terms of CCAAT recognition (Figure 2b). Ad-dnYA injection resulted in almost complete inhibition of luciferase activity in every body area after 2 d, returning to almost basal level at day 8 (Figures 2c and S4). These results definitely demonstrate that the luciferase gene is expressed in an NF-Y–dependent manner in every area of the MITO-Luc mice.

The cellular distribution of NF-Y and luciferase was analyzed by immunohistochemistry (Figure 2d). Adjacent slices from testis, spleen, and, as a negative control, skeletal muscle, were stained with antibodies against NF-YA or luciferase. Immunoreactivity for both was clearly detected in testis and spleen, while no staining was observed in skeletal muscle. Both testis and spleen contain proliferating cells, while postmitotic cells are the main constituents of skeletal muscles. To detect proliferating cells, we stained the slices with the antibody anti-PCNA, an antigen expressed in proliferating cells and not in quiescent cells. As expected, PCNA is expressed in the proliferating germ cells and spermatogonium inside the seminiferous tubules of the testis, and in several cells in the spleen. Of note, cells expressing the proliferation marker PCNA contain high levels of NF-YA and luciferase, indicating that in live animals, as in cultured cells, the NF-Y complex is active in proliferating, but not in postmitotic, cells. Most notably, the results in Figures 1 and 2 point to the MITO-Luc reporter mice as a powerful tool for visualizing proliferation events in live animals.

#### Analysis of luciferase activity upon inhibition of proliferation in MITO-Luc mice

To further understand whether the luciferase activity does occur in proliferating cells, we treated MITO-Luc mice with 5-fluorouracil (5-FU), a well-known antiproliferative drug (Hofer *et al.*, 2006). The main effects of 5-FU are on rapidly proliferating tissues, particularly bone marrow. After 5 d of treatment, we collected bone marrow from MITO-Luc mice femurs and observed that the luciferase activity was strongly inhibited by the drug treatment (Figure 3a). This inhibition correlates well with the inhibition of the S phase of bone marrow cell mediated by the drug treatment, as observed by fluorescence-activated cell sorting (FACS) analysis (Figure 3b). We next observed the effects of 5-FU in a long-term experiment. We monitored the

drug effects over time, reimaging the same animal at various time points posttreatment. Representative images are shown at 5, 10, 15, 23, 30, and 75 d posttreatment (Figure 3c). In the first 5 d after treatment, we observed a significant decrease of luminescence over the entire body. Fifteen days later, we observed luminescence in the spleen, which indicated that proliferation was occurring in the tissue at that time, and it is already known that spleen cells proliferate at this time to repopulate the bone marrow. Whole-body luminescence was completely restored at 75 d posttreatment. It has been shown that ionizing irradiation of normal tissues leads to tissue damage through cell cycle arrest and apoptosis (Stone *et al.*, 2003). Thus MITO-Luc mice were subjected to whole-body cesium  $\gamma$ -irradiation with sublethal doses of 3 and 5 Gy. Baseline images were obtained before treatment, and mice were then reimaged at various time points

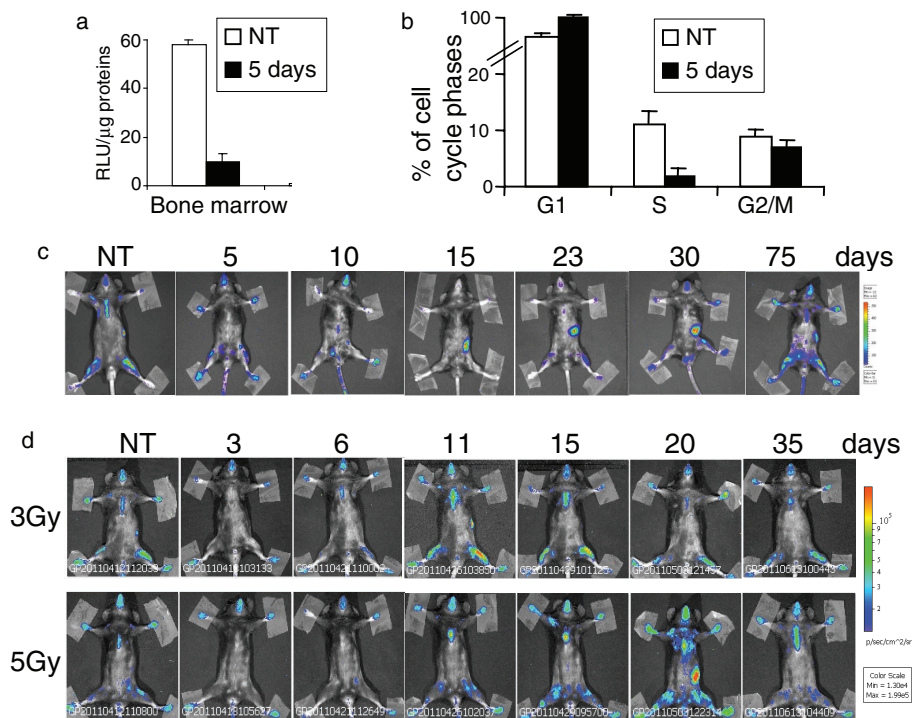


**FIGURE 3:** Analysis of luciferase activity upon inhibition of proliferation in MITO-Luc mice. (a) In vitro luciferase activity and (b) FACS analysis of MITO-Luc mouse bone marrow 5 d after treatment with 5-FU antiproliferative drug (150 mg/kg). Error bars represent the deviation of the mean of bone marrow from three animals. (c) BLI of a representative MITO-Luc mouse before (NT) and after (5, 10, 15, 23, 30, and 75 d) treatment with 5-FU (150 mg/kg). The experiments were conducted in five animals. (d) BLI of a representative MITO-Luc mouse before (NT) and after (3, 6, 11, 15, 20, and 35 d) treatment with 3 or 5 Gy. The experiments were conducted in five animals. (c and d) Light emitted from the animal appears in pseudocolor scaling.

posttreatment. Representative images are shown at 3, 6, 11, 15, 20, and 35 d posttreatment (Figure 3d). At 3 d posttreatment, luciferase activity was inhibited in the entire body, indicating that both radiation doses induced tissue damage. At 11 and 20 d, in mice treated with 3 and 5 Gy, respectively, we observed an increase of luciferase activity, indicating that tissue repair mediated by proliferation was occurring at those times. In both cases, luminescence declined to the baseline until 35 d posttreatment. Taken together, these data strongly support the idea that luciferase activity maps whole-body proliferation events in MITO-Luc mice.

### Luciferase activity is high in proliferating cells derived from MITO-Luc mice

We observed high luciferase activity in MITO-Luc mouse embryos at 19 d postcoitum (dpc; Figure 4a). Luciferase activity was analyzed in embryonic tissues at 19 dpc and found present in all, although to different extents (Figure 4b). Since cell proliferation is widespread in embryonic tissues, these results support the hypothesis that NF-Y activity in intact animals correlates with this process. We have previously demonstrated that NF-Y exerts its transcriptional activity in primary proliferating myoblasts and fibroblasts but is inactive in terminally differentiated myotubes and quiescent fibroblasts (Gurtner *et al.*, 2008). We asked whether NF-Y was active in primary proliferating myoblasts from MITO-Luc mice. Figure 4c shows that luciferase activity is high in primary myoblasts obtained from skeletal muscles of newborn MITO-Luc mice, while it is shut down in terminally differentiated myotubes. As a control for proliferation, myoblasts and myotubes were cultured for 24 h in the presence of BrdU, a marker

of DNA synthesis, and were then immunostained for BrdU. As expected, 95% of the myoblasts incorporated BrdU, while myotubes did not. As a control, myoblasts and myotubes were immunostained for muscle-specific myosin heavy chain (MHC), a marker of terminal differentiation in skeletal muscle. As expected, the majority of the myotubes expressed MHC, while myoblasts did not. Next, mouse embryonic fibroblasts (MEFs) were isolated from MITO-Luc mice and, as shown in Figure 4d, luciferase activity was high in proliferating MEFs, but was shut down in quiescent MEFs. Moreover, activity was greatly down-regulated in MEFs at 24 h postinfection with Ad-dnYA (Figure S5). These results demonstrate that the luciferase gene is expressed in an NF-Y-dependent manner in proliferating cells isolated from MITO-Luc mice. Moreover, these results also give information about the leakage of the transgene. Indeed, both in myotubes and in quiescent fibroblasts the luciferase activity is very low, suggesting that the expression of the luciferase is not influenced by the surrounding chromatin.

### Luciferase activity is induced in MITO-Luc mouse tissues upon induction of proliferation

We asked whether it was possible to induce luciferase expression upon induction of proliferation in MITO-Luc mice. Aberrant proliferation represents an early occurring pro-

neoplastic event. We therefore induced formation of skin papillomas by local administration of 7,12-dimethylbenz(a)anthracene and phorbol ester 12-O-tetradecanoylphorbol-13 acetate (DMBA-TPA) to the skin of MITO-Luc mice. DMBA and TPA were put directly onto shaved ventral skin (Figure 5a), with DMBA applied once-weekly and TPA applied twice-weekly. Representative images are shown for 2, 4, 6, and 8 wk after the first DMBA treatment. We detected luminescence at the treated sites directly after the first DMBA application and during the DMBA-TPA treatment period prior to tumor occurrence, which took place between 12 and 14 wk after treatment. Quantification of luminescence detected at different time points is shown in Figure 5b. The same results were achieved by applying the DMBA-TPA protocol to the mouse ear. Representative images are shown at 1, 2, 4, 5, 7, 10, 11, 12, and 14 wk after the first DMBA treatment (Figure 5c), and data are presented graphically in Figure 5d.

We next asked whether induction of luciferase expression upon induction of proliferation/regeneration is a general feature of MITO-Luc mouse tissues. We analyzed the light emitted by skeletal muscle during regeneration following acute hind limb ischemia. This rapid repair process is mainly carried out by satellite cells (SCs) that become active and proliferate upon injury (Zaccagnini *et al.*, 2007). Unilateral hind limb ischemia was induced in MITO-Luc mice by removing the femoral artery. As shown in Figure S6A, light emission decreased in the injured limb at 1 d postischemia, compared with the contralateral limb, which emitted light from the femur and bone marrow (Figure 1c). Of note, at 2, 4, and 7 d postischemia, adductor and gastrocnemius muscles from injured limb emitted light, as demonstrated by in vitro luciferase assays in protein extracts from these

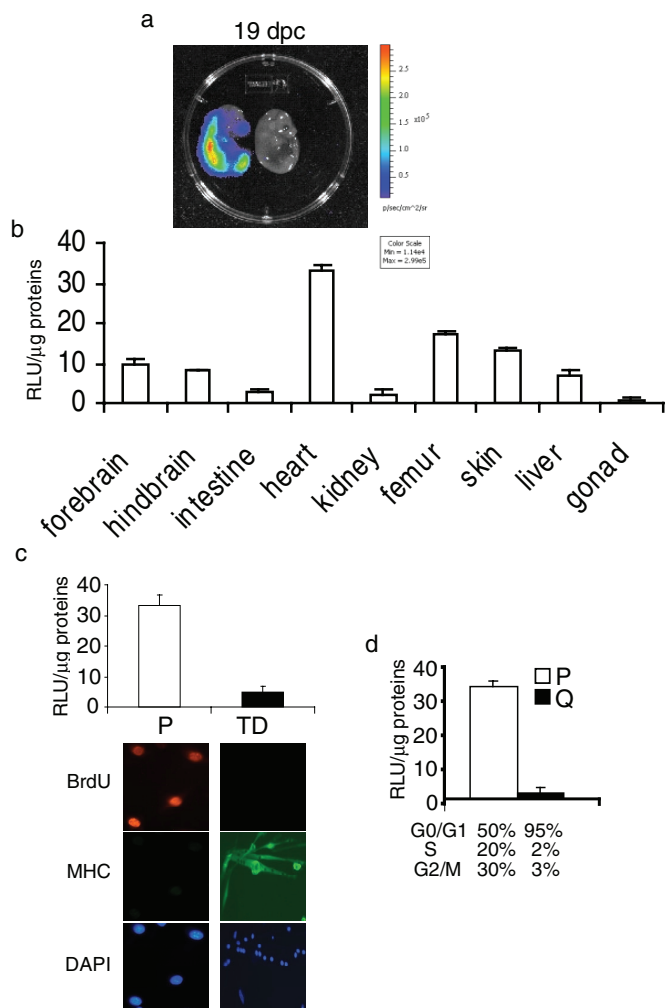


**FIGURE 4:** Luciferase activity in MITO-Luc mouse embryos and derived cells. (a) BLI of a representative MITO-Luc embryo at 19 dpc. Both positive and negative littermates are shown. The luciferase activity is visualized in pseudocolor scaling. (b) *in vitro* luciferase activity in tissues of 19 dpc MITO-Luc embryos. Each bar represents the mean value  $\pm$  SEM of three to six embryos. (c) *In vitro* luciferase activity in proliferating myoblasts (P) or terminal differentiated myotubes (TD) derived from newborn MITO-Luc mice. Immunofluorescence to detect MHC or BrdU incorporation is shown. Nuclei were visualized with DAPI. (d) Luciferase activity in proliferating (P) or quiescent (Q) MITO-Luc mouse embryonic fibroblasts. Percentage of cell cycle phase distribution of P and Q cells is reported. Values are the mean of two experiments performed in triplicate.

tissues (Figure S6B). Part of the light in this and the contralateral limb originated from the femoral bone marrow (Figure S6C).

Finally, we took advantage of a regeneration model after hepatic injury with carbon tetrachloride (CCl<sub>4</sub>) administration. During regeneration of mammalian liver, quiescent hepatocytes reenter the cell cycle and divide synchronously once or twice before returning to quiescence (Fausto, 2000). This process is concomitant with transcriptional induction of several NF- $\kappa$ B target genes regulating cell proliferation, for example, members of the *cyclin* and *cdk* families. Using *in vivo* (Figure 6a), *ex vivo* (Figure 6b), and *in vitro* (Figure S7) BLI experiments, we observed that CCl<sub>4</sub>-induced liver injury resulted in transient luciferase activation in the liver of MITO-Luc mice, peaking at 4 d after treatment and returning to almost basal level after 6 d. Staining of adjacent slices from livers of CCl<sub>4</sub>-treated mice with

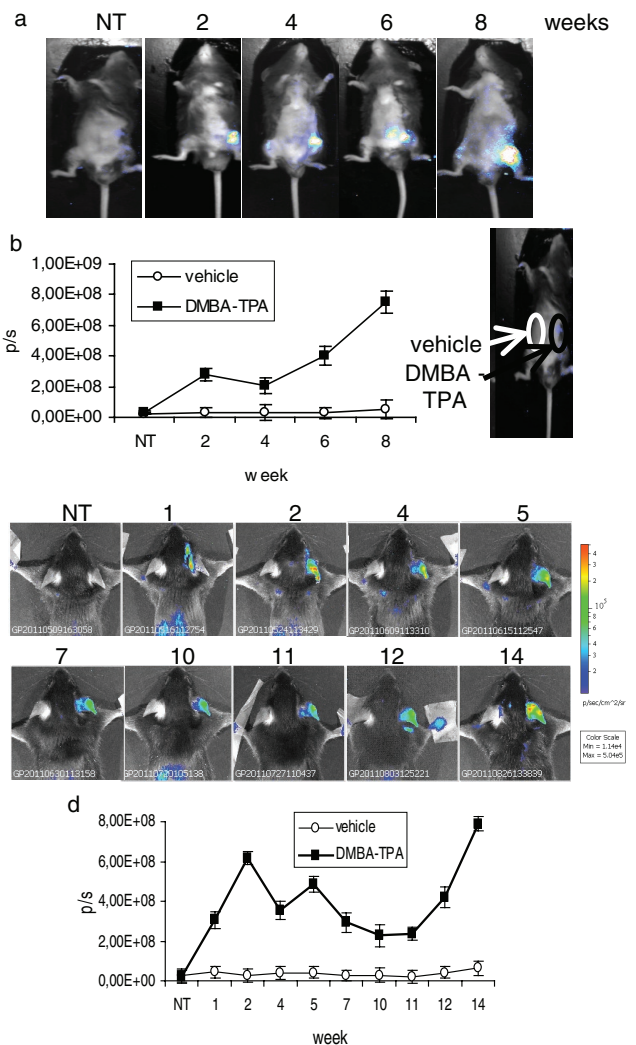


**FIGURE 5:** Luciferase activity in MITO-Luc mouse-induced papillomas. (a) BLI of a representative MITO-Luc mouse after 2, 4, 6, and 8 wk of DMBA-TPA treatments on ventral skin. (b) Quantification of emitted light from MITO-Luc mouse skin papillomas. The sites on the ventral surface of the animals in which the vehicle and the DMBA-TPA drugs have been spotted are indicated. (c) BLI of a representative MITO-Luc mouse after 1, 2, 4, 5, 7, 10, 11, 12, and 14 wk of DMBA-TPA treatments on mouse ear. (d) Quantification of emitted light from MITO-Luc mouse ear papillomas. (a and c) Light emitted from the animal appears in pseudocolor scaling. (b and d) Photon emission from the lesions (black square) and from the contralateral part (white circle) measured as photons per second (p/s). Each bar represents the mean value  $\pm$  SEM of four animals.

antibodies against PCNA or luciferase showed significant overlap in the expression of both markers (Figure 6c).

Luciferase activity was not present in CCl<sub>4</sub>-treated MITO-LUC mouse liver pretreated with a cobra toxin, MCTX (Figure 6e), which impairs entry of hepatocytes into S phase. Moreover, Ad-dnYA injection in CCl<sub>4</sub>-treated mice strongly inhibited luciferase activation in liver, compared with luciferase activation observed in mice injected with an adenovirus carrying a wild-type NF- $\kappa$ B protein (Ad-NFYA), as demonstrated by *in vivo* (Figure 7a) and *ex vivo* (Figure 7b) BLI and *in vitro* experiments (Figure 7c). As expected, an empty adenovirus, used as a control, showed intermediate luciferase activation (unpublished data). Of note, the Ad-dnYA effect was accompanied by a

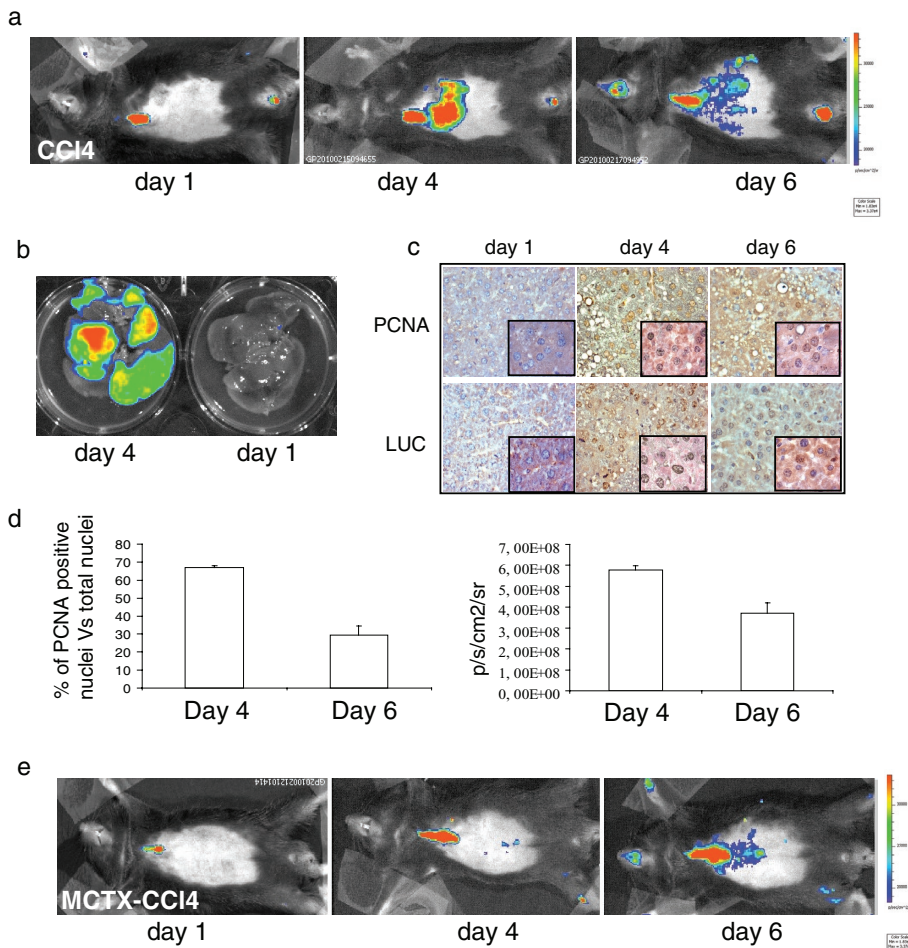


**FIGURE 6:** Luciferase activity during MITO-Luc mouse tissue regeneration. (a) BLI of a representative MITO-Luc mouse after 1, 4, and 6 d of CCl<sub>4</sub>-induced liver damage. After fur removal in the ventral region, the images were collected in a ventral close-range mode. (b) Ex vivo optical imaging of a MITO-Luc mouse liver damaged by CCl<sub>4</sub>. (c) Immunohistochemical analysis of PCNA and luciferase (LUC) in liver tissue from a representative MITO-Luc mouse damaged by CCl<sub>4</sub>. Images were collected at 40× (insets: 100×). (d) Quantification of PCNA-positive nuclei in liver tissue sections (left graph) and quantification of liver photon emission (right graph) at days 4 and 6 after liver injury. Error bars indicate the deviation of the mean of two experiments performed in triplicate. (e) BLI of a representative MITO-Luc mouse after 1, 4, and 6 d of treatment with MCTX and CCl<sub>4</sub>. (a, b, and e) Experiments were conducted in five animals per group.

strong reduction of a well-known NF-Y target gene, *cyclin A*, during cell cycle progression, demonstrating that the luciferase inhibition in the liver of Ad-dnYA-injected mice is due to inhibition of proliferation (Figure 7d). These results indicate that induction of luminescence strictly correlates with induction of proliferation in MITO-Luc mice and strongly suggest that NF-Y activity is essential for hepatocyte proliferation during liver regeneration in intact animals.

## DISCUSSION

In the present study, we generated a reporter transgenic mouse model in which, using the activity of the master regulator of proliferation, NF-Y, it is possible to visualize proliferation in intact animals. As a sensor of NF-Y transcriptional activity, we used a cyclin B2 promoter fragment to drive the transcription of the luciferase gene. We demonstrated that luciferase activity is strictly NF-Y-dependent by using a dominant-negative protein for NF-Y that completely abolishes luciferase activity in these mice. Thus the new transgenic mouse model, called MITO-Luc reporter mouse, is an unprecedented tool for fol-

lowing NF-Y transcriptional activity in vivo. Notably, the fact that NF-Y activity is exerted only in proliferating cells provides the unprecedented ability to follow physiological and/or pathological proliferation in every body area of these mice. Specifically, we observed by in vivo, ex vivo, and in vitro experiments that luciferase activity in adult mice is high in tissues containing proliferating cells, while tissues that do not show luciferase activity are mainly constituted by growth-arrested and/or postmitotic cells.

The pattern of luciferase activity in MITO-Luc reporter mice appears to be highly stable and reproducible. Indeed, from F1 to the current F13 generation, we have imaged ~300 mice and no differences have been observed. Thus MITO-Luc mice appear to be a reproducible system for imaging proliferation events in vivo. However, our ex vivo experiments indicate that some luminescence is lost due to tissue penetration. In addition to attenuation of light by overlying tissues, BLI is decreased by fur pigmentation. All BLI experiments shown here were performed after removal of fur with a depilatory agent. We have now bred MITO-Luc mice into FVB mice, and in this new animal model, we have been able to reproduce the phenotype observed in C57BL/6 mice without removing the fur (Manni, personal communication). Interestingly, we have demonstrated that the number of proliferating cells, counted as PCNA-positive cells, parallels photon emission in vivo (Figure 6d). We now have preliminary results on the sensitivity of this reporter system that indicate BLI detects proliferation events in MITO-Luc mice more efficiently than does staining with a marker of cell proliferation (unpublished data).

Induction of luciferase activity occurs in MITO-Luc mice tissues when proliferation is induced. As proof of principle, we induced skin papillomas in MITO-Luc mice, and we detected luminescence at the treated sites several days before tumor appearance, which indicates that the MITO-Luc animal model will allow study of early tumor development by noninvasive imaging techniques. Moreover, we demonstrated that proliferation events during muscle regeneration after femoral ischemia, as well as during liver regeneration after drug injury, are detectable by the IVIS Imaging System. Thus we now have evidence not only in culture cells but also in intact animals that the NF-Y complex exerts its activity in proliferating cells and not in postmitotic ones. Moreover, using a dominant-negative protein of NF-Y, we demonstrated for the first time that not only is NF-Y activity induced during liver regeneration after drug injury, but it is also essential for it.

Many pathological and physiological processes involve changes in cell proliferation. For the most part, this has been followed at the tissue and cellular level in collected samples. Recently the generation of the Fucci system (Sakaue-Sawano *et al.*, 2008) enabled cell cycle analysis to be efficiently carried out at the organismal level. However, this again is restricted to nonvital samples, and the utility of this model for

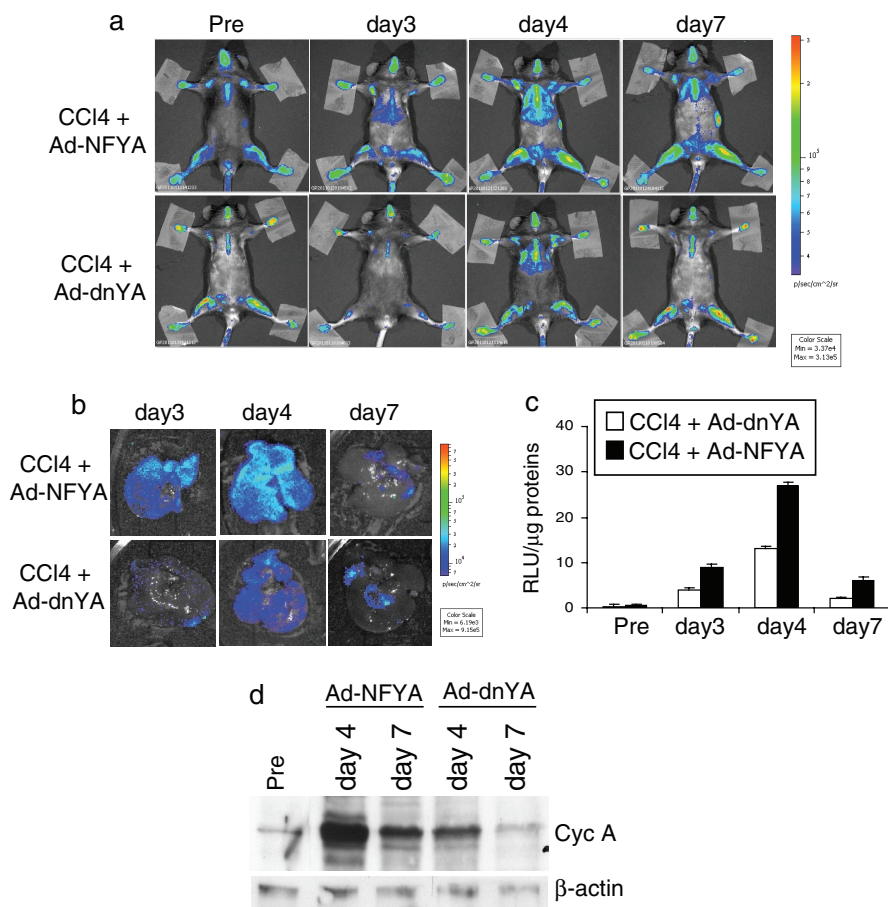


**FIGURE 7:** NF-Y activity during liver regeneration. (a) BLI of a representative MITO-Luc mouse after CCl<sub>4</sub>-treatment and intravenous injection of Ad-NFYA or Ad-dnYA. Experiments were conducted in six animals per group. (b) Ex vivo BLI of representative MITO-Luc mouse livers after intravenous injection of Ad-NFYA or Ad-dnYA and CCl<sub>4</sub> treatment at the indicated time points. (c) In vitro luciferase activity in liver after intravenous injection of Ad-NFYA or Ad-dnYA and CCl<sub>4</sub> treatment. Each bar represents the mean value ± SEM of three animals. (d) Western blot analysis of cyclin A expression in livers from MITO-Luc mice after CCl<sub>4</sub>-treatment and intravenous injection of Ad-NFYA or Ad-dnYA. β-actin has been used as loading control.

studying cell proliferation in adult animals has not been shown, whereas the mouse model we have developed enabled monitoring of cell proliferation in live animals. MITO-Luc mice crossed with animal disease models will allow study of aberrant proliferation in a given pathogenesis in the entire animal. Further, MITO-Luc mice will enable cancer imaging during and after therapy and will open up new possibilities for the study in live organisms of drugs affecting proliferation.

## MATERIALS AND METHODS

### Plasmid generation

We used a described vector, pHS4, for the generation of the MITO-Luc reporter constructs (Ciana *et al.*, 2003) using standard cloning procedures. The constructs, pHS4wtB2-luc and pHS4mutB2-luc, were obtained by cloning a murine cyclin B2 promoter fragment into the NdeI and BglII sites of the pHS4 plasmid. This murine cyclin B2 promoter fragment spans the -266 to +46 base-pair region with respect to the transcription start site in front of a luciferase reporter with wild-type or mutant NF-Y-binding sites.

### Generation and genotyping of the transgenic mice

The transgene was isolated from the vector backbone, and the purified fragment was injected into pronuclear DNA of fertilized

C57Bl/6xDBA/2 eggs using a standard protocol (Hogan *et al.*, 1994). Injected zygotes were reimplanted into pseudopregnant B6D2F1 (C57Bl/6xDBA/2) foster mothers to complete their development. The lineages were maintained in the heterozygous state. After genomic DNA extraction of tail biopsies (Ciana *et al.*, 2003), the positive founder animals were identified by PCR using the following primers specific for the transgene: oligonucleotide up: 5'-TG TAGACAAGGAAACAACAAAGCCTGTGGCC; and oligonucleotide down: 5'-GGCGTCTTCCATTTTACCAACAGTACCGG.

### In vivo and ex vivo BLI

Light emission was detected using the IVIS Lumina II CCD camera system and analyzed with the Living Image 2.20 software package (Caliper Life Sciences). Mice were anesthetized and 150 or 75 mg/kg of D-luciferin was injected intraperitoneally. Ten minutes later, quantification of light emission was performed in photons/second and visualized in a pseudocolor scaling. Time exposure ranged from 1 to 5 min, depending on light intensity.

### Luciferase assay from tissue extracts

After tissue dissection, the organs were immediately frozen on dry ice. Bone marrow was flushed out from the femur and tibia, as previously described (Gurtner *et al.*, 2010). Tissue extracts were prepared by homogenization in a 100 mM KPO<sub>4</sub> lysis buffer (pH 7.8) containing 1 mM dithiothreitol, 4 mM ethylene glycol tetraacetic acid, 4 mM EDTA, and 0.7 mM phenylmethylsulfonyl fluoride. After three freeze-thaw cycles, the extracts were centrifuged, the supernatants were collected, and the protein concentration was determined by Bradford's assay. Luc assay was performed according to Manni *et al.* (2001). The values were normalized for β-galactosidase expression and/or protein amounts.

### Immunohistochemistry

Serial sections of MITO-Luc mice tissues were prepared as previously described (Gurtner *et al.*, 2003). Primary antibodies were: 5 μg/100 μl anti-NF-YA (Rockland), 2 μg/100 μl anti-PCNA 19A2 (Beckman Coulter, Brea, CA), and an anti-luciferase (1:1800 dilution in phosphate-buffered saline with 10% goat serum and 0.3% Triton [Sigma-Aldrich, St. Louis, MO]). Sections were processed following the manufacturer's instruction of the UltraTek HRP Anti-Polyvalent (DAB) Staining System (Scytek). Peroxidase activity of the tertiary antibodies was visualized by reaction with 3,3'-diaminobenzidine and H<sub>2</sub>O<sub>2</sub> in sodium phosphate buffer (Vector Laboratories, Burlingame, CA). The sections were stained with hematoxylin.

### Cell culture and transfections

C2C12 cells were cultured and transiently transfected as previously described (Manni *et al.*, 2001). Primary myoblasts were isolated from mouse embryos and maintained and induced to differentiate

(myotubes) in culture as previously described (Gurtner *et al.*, 2008). MEFs were isolated and cultured from 13.5-d-old embryos as previously described (Gurtner *et al.*, 2010).

### Cell cycle analysis

DNA distribution analysis of propidium iodide-stained cells was performed according to standard procedures. A total of 10<sup>4</sup> events were analyzed by a cytofluorometer (Beckman Coulter). Cell cycle distribution was determined using computer-assisted analysis (M-cycle software).

### Pharmacological and surgical treatments

Ventral and ear skin papillomas were generated following a DMBA-TPA protocol. Briefly, mice were treated with a single topical application of 860  $\mu$ M DMBA (Sigma-Aldrich) in 0.2 ml acetone or with the solvent alone on their shaven skin or ears. One week after, 100  $\mu$ M of TPA (Alexis Biochemicals, San Diego, CA) in 0.2 ml acetone or the solvent alone was topically applied twice-weekly to the skin or ears. The surgical procedure for creating unilateral hind limb ischemia was performed according to Zaccagnini *et al.* (2007). Acute hepatic injury was obtained by intraperitoneal single injection of CCl<sub>4</sub> (1 ml/kg; Sigma-Aldrich) dissolved in peanut oil (Pilichos *et al.*, 2004). Monocrotaline (MCTX; Sigma-Aldrich) treatment was performed according to standard procedures (Witek *et al.*, 2005). The recombinant adenovirus vectors expressing green fluorescent protein (GFP), NFYA, and dn-YA (Gurtner *et al.*, 2008) were injected into the tail vein in adult mice. Mice were treated intravenously with 150 mg/kg of 5-FU (Teva Pharma Italia, Milan Italy). For irradiation experiments, mice were placed in the chamber and whole-body-irradiated with 3–5 Gy of  $\gamma$ -rays from a CIS BioInternational IBL 437C <sup>137</sup>Cs gamma.

### Immunofluorescence

Cells were stained with Anti-BrdU (clone B44; BD Bioscience) and MHC (mouse hybridoma; Magenta *et al.*, 2003) primary antibodies and Cy3- and Cy5-conjugated donkey anti-mouse as secondary antibodies (Jackson ImmunoResearch, West Grove, PA). Nuclei were stained with 4',6-diamidino-2-phenylindole (DAPI; 33258; Sigma-Aldrich).

### Experimental animals

Animal experiments performed in this study were conducted according to the "Guidelines for Care and Use of Experimental Animals" and the Italian law DL 116/92.

### ACKNOWLEDGMENTS

We thank Maria Pia Gentileschi for technical advice, Daniela Bona for secretarial assistance, Deborah Pajalunga for embryo muscle satellite purification, and the Regina Elena Institute animal house for mouse breeding. We are grateful to Beatrice David for the technical support for the *in vivo* imaging. This work has been partially supported by grants from AIRC and Ministero della Salute (ICS-120.4/RA00-90; R.F.02/184) to G.P., Cariplo Foundation (grant no. 2009-2439) to P.C. and G.P., and financial support of the European Community IP project EPITRON LSHC CT 2005 512146 to A.M. F.G. was supported by a postdoctoral fellowship from the DAAD (German Academic Exchange Service). S.A. is supported by Fondazione Umberto Veronesi. This article is dedicated to the memory of Cecilia Tiveron.

### REFERENCES

Bhattacharya A, Deng JM, Zhang Z, Behringer R, de Crombrughe B, Maity SN (2003). The B subunit of the CCAAT box binding transcription factor complex (CBF/NF-Y) is essential for early mouse development and cell proliferation. *Cancer Res* 63, 8167–8172.

Bolognese F *et al.* (1999). The cyclin B2 promoter depends on NF-Y, a trimer whose CCAAT-binding activity is cell-cycle regulated. *Oncogene* 18, 1845–1853.

Bungartz G, Land H, Scadden DT, Emerson SG (2012). NF-Y is necessary for hematopoietic stem cell proliferation and survival. *Blood* 119, 1380–1389.

Caretti G, Motta MC, Mantovani R (1999). NF-Y associates with H3-H4 tetramers and octamers by multiple mechanisms. *Mol Cell Biol* 19, 8591–8603.

Ciana P, Raviscioni M, Mussi P, Vegeto E, Que I, Parker MG, Lowik C, Maggi A (2003). *In vivo* imaging of transcriptionally active estrogen receptors. *Nat Med* 9, 82–86.

Di Agostino S, Strano S, Emiliozzi V, Zerbini V, Mottolese M, Sacchi A, Blandino G, Piaggio G (2006). Gain of function of mutant p53: the mutant p53/NF-Y protein complex reveals an aberrant transcriptional mechanism of cell cycle regulation. *Cancer Cell* 10, 191–202.

Dolfini D, Zambelli F, Pavesi G, Mantovani R (2009). A perspective of promoter architecture from the CCAAT box. *Cell Cycle* 8, 4127–4137.

Farina A, Manni I, Fontemaggi G, Tiainen M, Cenciarelli C, Bellorini M, Mantovani R, Sacchi A, Piaggio G (1999). Down-regulation of cyclin B1 gene transcription in terminally differentiated skeletal muscle cells is associated with loss of functional CCAAT-binding NF-Y complex. *Oncogene* 18, 2818–2827.

Fausto N (2000). Liver regeneration. *J Hepatol* 32, 19–31.

Grskovic M, Chaivorapol C, Gaspar-Maia A, Li H, Ramalho-Santos M (2007). Systematic identification of cis-regulatory sequences active in mouse and human embryonic stem cells. *PLoS Genet* 3, e145.

Gurtner A, Fuschi P, Magi F, Colussi C, Gaetano C, Dobbstein M, Sacchi A, Piaggio G (2008). NF-Y dependent epigenetic modifications discriminate between proliferating and postmitotic tissue. *PLoS One* 3, e2047.

Gurtner A *et al.* (2010). Transcription factor NF-Y induces apoptosis in cells expressing wild-type p53 through E2F1 upregulation and p53 activation. *Cancer Res* 23, 9711–9720.

Gurtner A, Manni I, Fuschi P, Mantovani R, Guadagni F, Sacchi A, Piaggio G (2003). Requirement for down-regulation of the CCAAT-binding activity of the NF-Y transcription factor during skeletal muscle differentiation. *Mol Biol Cell* 14, 2706–2715.

Hofer M, Pospisil M, Vacek A, Holá J, Znojil V, Weiterová L, Streitová D (2006). Effects of adenosine A3 receptor agonist on bone marrow granulocytic system in 5-fluorouracil-treated mice. *Eur J Pharmacol* 538, 163–167.

Hogan B, Beddington R, Costantini F, Lacey E (1994). *Manipulating the Mouse Embryo: A Laboratory Manual* 2nd ed., Cold Spring Harbor, NY: Cold Spring Harbor Press.

Magenta A, Cenciarelli C, De Santa F, Fuschi P, Martelli F, Caruso M, Felsani A (2003). MyoD stimulates RB promoter activity via the CREB/p300 nuclear transduction pathway. *Mol Cell Biol* 23, 2893–2906.

Manni I, Caretti G, Artuso S, Gurtner A, Emiliozzi V, Sacchi A, Mantovani R, Piaggio G (2008). Posttranslational regulation of NF-YA modulates NF-Y transcriptional activity. *Mol Biol Cell* 19, 5203–5213.

Manni I, Mazzaro G, Gurtner A, Mantovani R, Haugwitz U, Krause K, Engeland K, Sacchi A, Soddu S, Piaggio G (2001). NF-Y mediates the transcriptional inhibition of the *cyclin B1*, *cyclin B2*, and *cdc25C* promoters upon induced G2 arrest. *J Biol Chem* 276, 5570–5576.

Mantovani R, Li XY, Pessara U, Hooft van Huisjdijnen R, Benoist C, Mathis D (1994). Dominant negative analogs of NF-YA. *J Biol Chem* 269, 20340–20346.

Pilichos C, Perrea D, Demonakou M, Preza A, Donta I (2004). Management of carbon tetrachloride-induced acute liver injury in rats by syngeneic hepatocyte transplantation in spleen and peritoneal cavity. *World J Gastroenterol* 10, 2099–2102.

Sakaue-Sawano A *et al.* (2008). Visualizing spatiotemporal dynamics of multicellular cell-cycle progression. *Cell* 132, 487–498.

Sciortino S, Gurtner A, Manni I, Fontemaggi G, Dey A, Sacchi A, Ozato K, Piaggio G (2001). The cyclin B1 gene is actively transcribed during mitosis in HeLa cells. *EMBO Rep* 2, 1018–1023.

Signore A, Mather SJ, Piaggio G, Malviya G, Dierckx RA (2010). Molecular imaging of inflammation/infection: nuclear medicine and optical imaging agents and methods. *Chem Rev* 110, 3112–3145.

Stone HB, Coleman CN, Anscher MS, McBride WH (2003). Effects of radiation on normal tissue: consequences and mechanisms. *Lancet Oncol* 4, 529–536.

Witek RP, Fisher SH, Petersen BE (2005). Monocrotaline, an alternative to retrorsine-based hepatocyte transplantation in rodents. *Cell Transplant* 14, 41–47.

Zaccagnini G, Martelli F, Magenta A, Cencioni C, Fasanaro P, Nicoletti C, Biglioli P, Pelicci PG, Capogrossi MC (2007). p66(ShcA) and oxidative stress modulate myogenic differentiation and skeletal muscle regeneration after hind limb ischemia. *J Biol Chem* 282, 31453–31459.